BULLETIN OF THE CHEMICAL SOCIETY OF JAPAN, VOL. 45, 3048—3053 (1972)

Electrochemical Behaviour of the Lithiated Nickel Oxide Crystal

Hiroshi YONEYAMA and Hideo TAMURA

Department of Applied Chemistry, Faculty of Engineering, Osaka University, Yamadakami, Suita, Osaka

(Received November 26, 1971)

The electrochemical properties of lithiated nickel oxide were studied using a single-crystal (100) face and a sintered body. The *I–V* curves of the Fe^{2+}/Fe^{3+} system on the single-crystal electrode were almost the same as those on the sintered-body electrode when the electric resistivities of the crystals were equal. However, a high amount of charge was obtained at the sintered-body electrode compared with the single-crystal electrode when the crystals were oxidized anodically. The effect on these reaction rates of the space charge depletion layer formed on the electrode surface will be discussed. The dependence of the reaction rates on the electric resistivity of the crystal can be understood to a certain extent through this discussion.

Charge transfer reactions of some redox systems on sintered-body lithiated nickel oxide electrodes were studied previously[1], and it was concluded that the electric resistivity of the crystal influences the charge-transfer reaction rates. It was also found[2] that the resistivity of the crystal affects the quantity of higher-valency nickel oxides formed by anodic oxidation. It is often pointed out that the grain boundaries of the crystal act as peculiar defect sites, such as charge-trapping or -generating centers. According to Morin,[3] sintered-body nickel oxide contains cation vacancies, the number of which is influenced by the preparation conditions. Taking account of this information, the electrochemical behaviour of the crystal may be said to be influenced by the grain boundaries. One purpose of this paper is to present the difference in the electrochemical behaviour of lithiated nickel oxide between the single crystal and the sintered body. Another purpose is to discuss the electrochemical behaviour of the material from the semiconductor's point of view.

1) H. Yoneyama and H. Tamura, This Bulletin, **43**, 1603 (1970).

2) H. Yoneyama and H. Tamura, *ibid.*, **42**, 1795 (1969).

3) F. J. Morin, *Phys. Rev.*, **93**, 1199 (1954).

Experimental

Electrodes. The single-crystal lithiated nickel oxide was prepared by the method of Rouse and Weininger,[4] using commercial lithiated nickel oxide (Nakazumi Crystal Co. Ltd.). Electroless plating nickel was chosen as the electrical contact. The contact prepared by this method showed good ohmic behaviour. The electrode surface was the (100) face. The sintered-body lithiated nickel oxide electrode was prepared by a method described in a previous paper.[1] It was prepared by firing at 1350°C in the air. The distribution of the grain size of nickel oxide powder as a raw material is shown in Fig. 1; it was determined by the Andreasen pipet method. The electric resistivity of the electrode was estimated by means of the voltage drop between the end faces of the crystal.

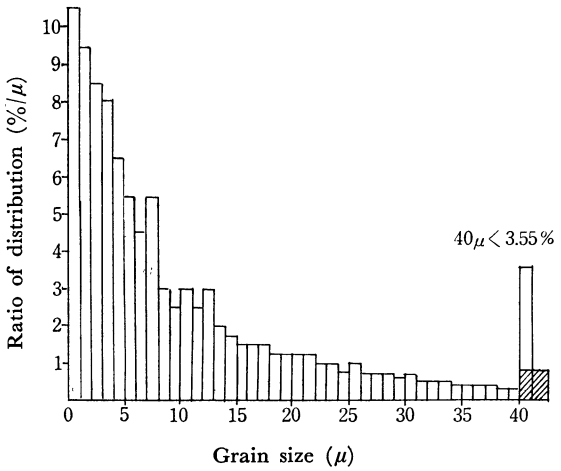

Fig. 1. Distribution of grain of NiO powder as a raw material.

Effective Surface Area of the Electorde. The effective surface area of the sintered-body electrode was determined by comparing the space charge capacitance of the depletion layer of the electrode with that of the single-crystal eleetrode in the following way.

Electrode surfaces of various single crystals and sintered bodies were polished with No. 2000 emery paper, followed by immersion in a mixed solution of conc. H_2SO_4 and conc. HNO_3 (1 : 1); then it was pretreated with a conc. HCl solution. After the electrode had been thoroughly washed with de-ionized water, the electric capacitance of the electrodes was measured in a 1N H_2SO_4 solution as a function of the electrode potential by means of the bridge arrangement shown in Fig. 2. Then the nominal carrier densities of various single-crystal electrodes were estimated usnig the relationship which can be applied for the depletion layer of the semiconductor:[5,6]

$$d(1/C^2)/dV = 2/(q\varepsilon\varepsilon_0 N) \quad (1)$$

In this equation, $q,\varepsilon,\varepsilon_0,N$, and C represent the elementary charge of the electron, the dielectric constant of the semiconductor, that of the vacuum, the carrier density of the semiconductor, and the capacitance of the depletion layer per unit of surface area of the semiconductor electrode. Typical examples are shown in Fig. 3. In the estimation of the nominal carrier densities of the various single crystals, the apparent geometric dimension was adopted as the effective surface area and the dielectric constant of the semiconductor was assumed to be 12.[7] Figure 4 shows the nominal carrier densities of the single-crystal electrodes as a function of their

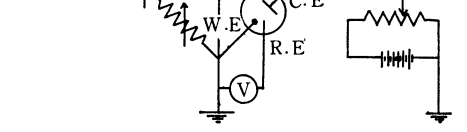

Fig. 2. Bridge arrangement for measurement of differential capacitance of electrode.

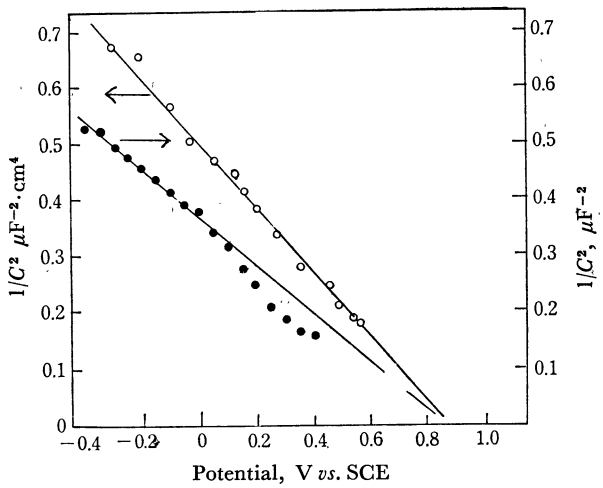

Fig. 3. Typical example of $1/C^2$ *vs.* V plot for two electrodes.
—●—: 580 Ω·cm sintered body, —○—: 580 Ω·cm single crystal.
solution: 1 N H_2SO_4

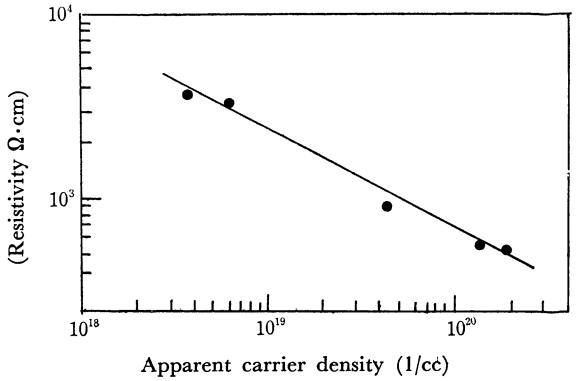

Fig. 4. Nominal carrier density as a function of resistivity of single crystal lithiated NiO.

4) T. O. Rouse and J. L. Weininger, *J. Electrochem. Soc.*, **113**, 184 (1966).

5) J. F. Dewald, *Bell System Tech. J.*, **39**, 615 (1960).

6) P. J. Boddy, *J. Electrochem. Soc.*, **115**, 199 (1968).

7) R. Newman and R. M. Chrenko, *Phys. Rev.*, **114**, 1507 (1959).

resistivities.[8]

Let it be assumed that the carrier density of the sintered body is eventually equal to that of the single crystal of the same resistivity. Then, the slope of the plots of $1/C^2$ *vs.* V should be equal to each other for the electrodes of the same resistivity when the effective areas of the electrodes are equal. The effective surface area of the sintered-body electrode was determined by correcting the area of the measured capacitance so as to have the same slope of $1/C^2$ *vs.* V plot as that of the single-crystal of the corresponding resistivity.

Measurement of I–V Curves and V–t Curves. *I–V* curves of the redox system were obtained potentiostatically. *V–t* curves during the anodic oxidation and cathodic reduction of the electrode were obtained by means of an electrometer connecting to a voltage recorder. Measurements were made for current densities in which the ohmic drop across the electrode could be almost negligible. Commercial dry nitrogen gas was bubbled into the electrolyte thermostated at 25±0.5°C during the measurements. Electrolytes were prepared by the use of reagent-grade chemicals and de-ionized water. The electrolytic cell was a conventional H-type cell.

Results

Redox Reaction of the Fe^{2+}/Fe^{3+} System. Figure 5 shows the anodic portions of the *I–V* curves of the Fe^{2+}/Fe^{3+} system (5×10^{-3} M Fe^{2+}, 5×10^{-3} M Fe^{3+}, in 1 N H_2SO_4) on single-crystal and sintered-body electrodes of the same resistivity. It is evident from this figure that no difference in the *I–V* curves can be observed between these two electrodes. The *I–V* curves of this system on various single-crystal electrodes are shown in Fig. 6.[9] The apparent exchange current

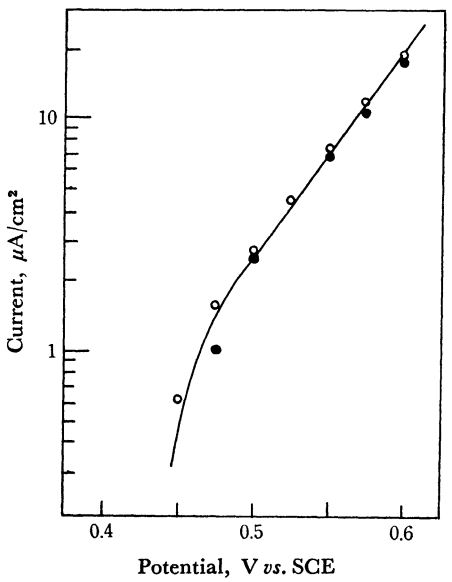

Fig. 5. Anodic portion of *I-V* curves of Fe^{2+}/Fe^{3+} system on sigle crystal and sintered body electrode having the same resistivity of 580 Ω·cm.
—●— sinterd body, —○— single crystal, solution: 5×10^{-3} M Fe^{2+}, 5×10^{-3} M Fe^{3+}/1 N H_2SO_4.

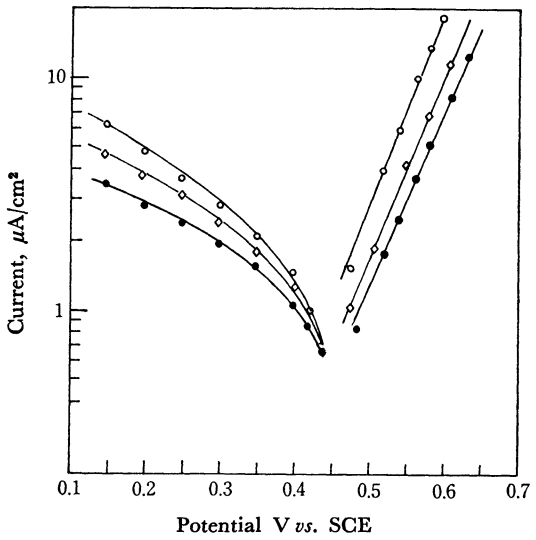

Fig. 6. *I-V* curves of Fe^{2+}/Fe^{3+} system on various single crystal electrodes.
—○— 580 Ω-cm, —◇— 1.6 kΩ-cm, —●— 3.8 kΩ-cm, solution: the same as in Fig. 5.

TABLE 1. APPARENT EXCHANGE CURRENT DENSITIES OF Fe^{2+}/Fe^{3+} SYSTEM ON VARIOUS SINGLE CRYSTAL ELECTRODES

Resistivity of electrode (Ω-cm)	580	1600	3800
Apparaent exchange current (A/cm²)	2.2×10^{-6}	1.1×10^{-6}	8.5×10^{-7}

Solution: 5×10^{-3} M Fe^{2+}, 5×10^{-3} M Fe^{3+} in 1 N H_2SO_4

densities of the system were estimated by the extrapolation of the anodic portion of the *I–V* curves in Fig. 6 to a redox potential of the system; they are shown in Table 1. According to Fig. 6, a linear slope was observed in the log I *vs.* V plot of the *I–V* curves of the anodic process, while the current showed a tendency to become saturated with the cathodic polarization. On the other hand, it can be seen in Table 1 that the exchange current densities of the system are influenced by the resistivity of the electrode. Such observations have previously been reported[1] for sintered-body electrodes. Therefore, they seems to be connected with the genuine properties of the lithiated nickel oxide.

Anodic Oxidation. Figure 7 shows the electrode potential behaviour of various electrodes during the 1st oxidation and reduction cycle. 10 μA/cm² and 1 μA/cm² were chosen as the anodic and cathodic current densities respectively. In this figure, the effective area of the 25 Ω·cm sintered-body electrode was estimated by a different method.[1] The cathodic *I–V* curves obtained in the electrolyte into which oxygen gas was bubbling are also shown in Fig. 7 for two kinds of electrodes, that is, the 180 Ω·cm sintered body and the 64 Ω·cm single crystal. A plateau of the potential was observed in the cathodic *V–t* curves. This poten-

8) As has previously been observed by Rouse and Weininger, the nominal carrier density, as estimated from the $1/C^2$ *vs.* V plot, does not accord with the lithium content in the crystal. However, the use of this nominal carrier density in the estimation of the effective surface area of the sintered-body electrode will not introduce any trouble.

9) Judging from the *I-V* curves in a system of Ni–NiO–Ni, where V is the applied voltage between nickel contacts and where I is the current, the voltage drops across the crystal per 1 μA/cm² were as follows: 580 Ω·cm: 0.075 mV, 1.6 kΩ·cm: 0.34 mV 3.8 kΩ·cm: 0.36 mV. *I-V* curves which have been corrected on the basis of thse voltage drops are presented in Fig. 6.

tial which appeared in the oxygen-bubbling electrolyte was by far more noble than that in the nitrogen-bubbling electrolyte. Figure 7 shows that the oxygen gas pressure has no influence on the V–t curves in the reduction process before the plateau of the potential due to oxygen reduction appears. From a comparison of the V–t curves under oxygen-bubbling conditions with those under nitrogen-bubbling conditions, it may be expected that V–t curves during the reduction in the noble potential region, more noble, say, than 0V, are mainly the result of the charge retained by anodic oxidation.[10] Hence, it follows from Fig. 7 that the

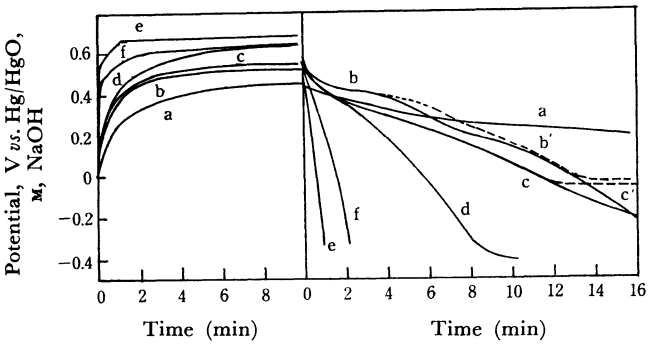

Fig. 7. Potential-time curves of various lithiated nickel oxide electrode during anodic and cathodic polarization.
anodic current density: 10 μA/cm^2, cathodic current density: 1μA/cm^2. solid line: in N_2 gas bubbling, dotted line: in O_2 gas bubbling, a: 25 Ω·cm, b: 64 Ω·cm single crystal, c: 180 Ω·cm. d: 580 Ω·cm, e: 580 Ω·cm single crystal, f: 2300 Ω·cm, b′: 64 Ω·cm single crystal, c′: 180 Ω·cm. solution: 1 M NaOH.

charge retained by anodic oxidation is high for an electrode of low resistivity. This conclusion is supported by the previous report[2] as well. Figure 7 suggests that the single crystal is less active in the anodic oxidation than the sintered body.

Discussion

Charge-transfer Reaction on the Lithiated Nickel Oxide Electrode. The rate equation of the charge-transfer reaction on the lithiated nickel oxide electrode will be presented first.

As only the positive hole participates in the charge-transfer process, the electrode reaction of the redox couple of Fe^{2+}/Fe^{3+} can be represented as[1];

$$Fe^{2+} + p \rightleftarrows Fe^{3+}$$

The positive hole concentration at the electrode surface, P_s, is related to the bulk concentration, P_b, according to the formulation by Myamlin and Pleskov[11]:

$$P_s = P_b \exp(F\psi_{sc}/RT) \quad (2)$$

where ψ_{sc} is the potential drop in the surface of the semiconductor and has a negative value when the space charge depletion layer is formed. The anodic current, J_a, and the cathodic current, J_c, can be expressed as:

$$J_a = kC_{Fe^{2+}}P_s \exp(\alpha F\psi_e/RT) = kC_{Fe^{2+}}P_b \times \exp(F\psi_{sc}/RT)\exp(\alpha F\psi_e/RT) \quad (3)$$

$$J_c = k'C_{Fe^{3+}}\exp(-\beta F\psi_e/RT) \quad (4)$$

where ψ_e is the potential drop in the Helmholtz double layer. The exchange current density, J_o, is:

$$J_o = kC_{Fe^{2+}}P_b \exp(F\psi_{sc}^\circ/RT)\exp(\alpha F\psi_e^\circ/RT) = k'C_{Fe^{3+}}\exp(-\beta F\psi_e^\circ/RT) \quad (5)$$

where ψ_{sc}° and ψ_e° are, respectively, the potential drop in the space charge layer of the electrode surface and that in the Helmholtz double layer when the electrode is in equilibrium with the redox couple. By substituting Eq. (5) into Eq. (3) and Eq. (4), we obtain:

$$J_a = J_0 \exp[\{F(\psi_{sc}-\psi_{sc}^\circ) + \alpha F(\psi_e-\psi_e^\circ)\}/RT] \quad (6)$$

$$J_c = J_0 \exp\{-\beta F(\psi_e-\psi_e^\circ)/RT\} \quad (7)$$

The potential drop in the Helmholtz double layer may be neglected when a distinct space-charge layer exists on the surface of the electrode. Then, ψ_{sc}° and ψ_{sc} relate to the flat-band potential, E_{fb}, the redox potential of the redox couple, E_{redox}, and the electrode potential, E, all of which are measurable values:

$$\psi_{sc}^\circ = E_{redox} - E_{fb} \quad (8)$$

$$\psi_{sc} = E - E_{fb} \quad (9)$$

In this case, the total current, J, is formulated as:

$$J = J_a - J_c = J_0 \exp\{(E-E_{redox})/RT - 1\} \quad (10)$$

In the above formulation, $C\mathrm{Fe}^{2+}$ and $C\mathrm{Fe}^{3+}$ are used as the concentrations of the ferrous and ferric ions in the electrolyte. The concentration of the redox couple at the energy level of the positive hole of the electrode surface is truly determined by the product of the concentration of the redox couple and the distribution function of the couple, which is approximately a function of the energy difference between the positive hole level at the electrode surface and the Fermi energy of the redox couple.[12] The effect of the distribution function on the charge-transfer reaction rate is contained in the rate constants, k and k' in Eq. (3) and Eq. (4) respectively.

Figure 3 suggests that the flat-band potential of the electrode in 1 N H_2SO_4 is 0.85 V *vs.* SCE, while Fig. 6 shows that the equilibrium potential of the redox couple and the electrode is by far less noble. Judging from these pieces of information, there must be a space-charge depletion layer on the surface of the electrode. Figure 8 shows an energy diagram[13] of the electrolyte/electrode interface; the potential drop in the Helm-

10) The difference in the charge value between this and the previous paper is due to the anodic oxidation conditions. In the previous experiments, the electrode had been exposed to a high anodic current density in the first oxidation cycle, while in the subsequent cycles the total charge supplied during the oxidation as well as the oxidation current density had not exceeded the value of the first cycle. For this reason, an almost constant charge was obtained regardless of the anodic oxidation conditions. In this sence, the previous description that the charge corresponding to the higher-valency nickel oxides formed by anodic oxidation is constant, regardless of the anodic oxidation current density, is inadequate. Hence, all the data presented previously should be understood to those for electrodes which had been exposed to the first oxidation conditions (10 mA/cm^2 × 5 min).

11) V. A. Myamlin and Yu. V. Pleskov, "Electrochemistry of Semiconductors," Plenum Press, New York (1967), p. 159.

12) H. Gerischer, *Surface Sci.*, **18**, 97 (1969).

13) The energy diagram presented in a previous paper (Ref. 1) contains a fault.

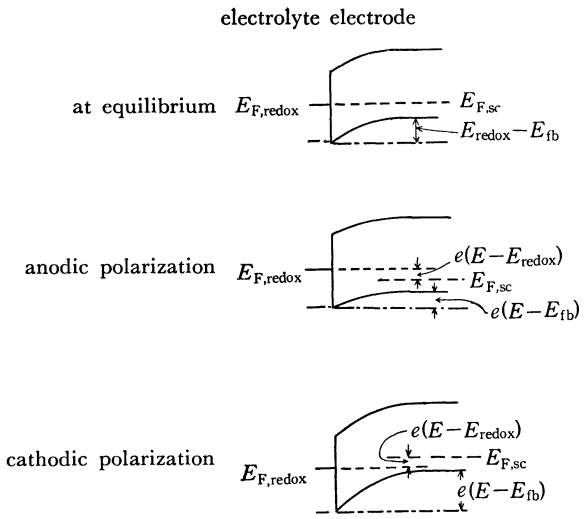

Fig. 8. Energy diagram of the electrode/electrolyte interface when the electrode contacts with a redox solution of Fe^{2+}/Fe^{3+} system.

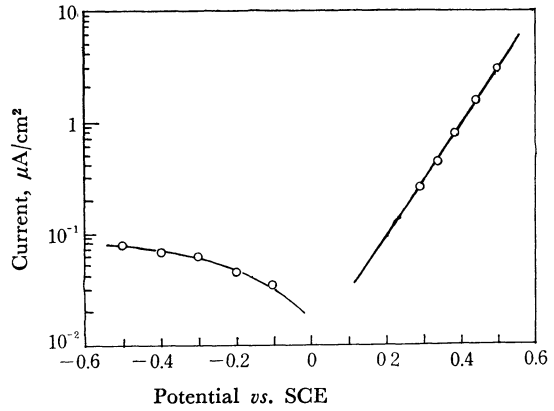

Fig. 9. *I-V* curves of Ti^{3+}/Ti^{4+} system in 1 N HCl solution on 580 Ω·cm single crystal electrode. Solution: 0.9 M Ti^{3+}, 0.1 M Ti^{4+} 1 N HCl.

holtz double layer is neglected. The solid lines of the energy diagram of the semiconductor shown in Fig. 8 denote the energy level of the positive hole and the electron respectively.[14,15] The experimental results which are shown in Fig. 6 for the Fe^{2+}/Fe^{3+} and in Fig. 9 for the Ti^{3+}/Ti^{4+} suggest that the ideal case, which is illustrated in Fig. 8, was not realized, for the anodic Tafel slope was not 59 mV/decade. However, the dependence of the exchange-current density on the resistivity of the electrode and the appearence of the Tafel slope in the anodic process can be understood by means of Eq. (5) and Eq. (6).

Anodic Oxidation. The charge retained by the anodic oxidation is possibly due to the formation of higher-valency nickel oxides. The phenomenon that the resistivity of the crystal affects this charge can not be explained on the basis of the atom arrangement of the crystal, since the dimensions of the unit cell decrease with increase in the lithium content.[16]

14) D. Adler, *Phys. Rev.* B, **2**, 3112 (1970).
15) S. van Houten, *J. Phys. Chem. Solid*, **17**, 7 (1960).
16) E. J. W. Verway, P. W. Haaijman, F. C. Romeijn, and G. W. van Osterhout, *Philips Res. Rept.*, **5**, 173 (1950).

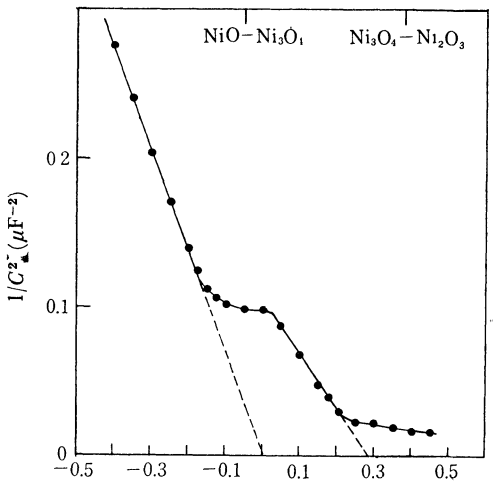

Fig. 10. $1/C^2$ *vs.* *V* plot for the sintered body of 580 Ω·cm. solution: 1 M NaOH, electrode area: 0.183 cm².

According to the above discussion, a potential drop in the space-charge depletion layer influences the electrochemical behaviour of the lithiated nickel oxide. Figure 10 shows the $1/C^2$ *vs.* *V* plot for the 580 Ω·cm sintered-body electrode in a 1 M NaOH solution. The thermodynamically-calculated equilibrium potentials of various nickel oxides[17] are also shown in this figure. Figure 10 clearly shows that the inflection of the $1/C^2$ vs. *V* plot occurs around the potential at which surface oxidation begins to occur, and that the flat-band potential shifts towards a more noble potential after beginning of surface oxidation. The shift of the flat-band potential towards a more noble potential may be brought about by the formation of the surface state, which is due to oxide formation. At any rate, Fig. 10 implies that there is a space-charge depletion layer on the electrode surface in the less noble potentials below 0.3 V (*vs.* Hg/HgO, M NaOH). According to Fig. 7, anodic oxidation proceeds to a certain extent in the potentials below 0.3 V. Therefore, the anodic oxidation mechanism below the flat-band potential will be discussed first.

When the space-charge layer exists on the electrode surface, the field strength across the space-charge layer will be different according to various resistivities of the electrode at the same polarization potential. The electric capacitance in Eq. (1) is related to the depth of the space-charge layer, *d*:

$$C = \varepsilon\varepsilon_0/d \qquad (9)$$

The potential drop in the space-charge layer corresponds ideally to the electrode potential as measured from the flat-band potential, $E-E_{fb}$. By replacing *V* in Eq. (1) with $(E-E_{fb})$ and by combining Eq. (1) with Eq. (9), we finally obtain the electric-field strength across the space-charge layer, which is shown in Eq. (10):

$$F = (E-E_{fb})/d = \{qN(E-E_{fb})/2\varepsilon\varepsilon_0\}^{1/2} \qquad (10)$$

Figure 11 shows the calculated field strength across

17) M. Pourbaix, "Atlas of Electrochemical Equilibria in Aqueous Solutions," Pergamon Press, Oxford (1966), p. 330.

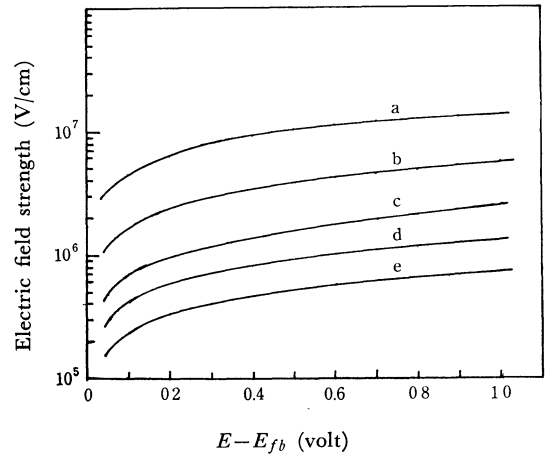

Fig. 11. Calculated electric field strength across the space charge in the electrode surface as a function of $E-E_{fb}$ a: 5.6 Ω·cm, b: 25 Ω·cm, c: 180 Ω·cm, d: 560 Ω·cm, e: 2300 Ω·cm.

the space-charge layer of the various electrodes as a function of $E-E_{fb}$. In the calculation, the value of N was estimated from the relationship between the lithium content and the resistivity of the crystal.[2] Figure 11 shows that the electric-field strength across the space-charge layer is high for the electrode of low resistivity.

The ionic current, I, in the anodic film formation process is generally expressed as:[18]

$$I = A \exp(\beta F) \tag{11}$$

where A and β are constants and where F is the electric-field strength. During the film formation process, an order of 10^6 V/cm is required for the value of F. According to Dewald's theoretical treatment of the mechanism of the formation of anodic oxide film at a high field,[19] there is a case where the contribution of the space charge layer to the F is predominate and where the rate of oxidation is determined almost entirely by the bulk properties of the film. If it is accepted that Dewald's theory is suitable for the anodic oxidation of the lithiated nickel oxide, it can be seen that the electrode of low-bulk resistivity suffers anodic oxidation more easily, although, in a strict sense, the precise estimation of various parameters in Dewald's theory is necessary in order to determine the applicability of the theory to this case.

The above mechanism of the anodic oxidation is probably restricted in the potential region below the flat-band potential, because the polarization potential is almost entirely concentrated in the Helmholtz double layer in the potential region above the flat-band potential of the electrode. The anodic oxidation above the flat-band potential will be influenced by the properties of the oxides formed by that time. Unfortunately, the properties of the oxides formed can not be elucidated at present becaue of its thinness.

Difference in Quantity of Higher-valency Oxides between Single Crystal and the Sintered Body. According to Fig. 7, the charge retained by the anodic oxidation seems to be different between the single crystal and the sintered body of the same resistivity. If the anodic oxidation mechanism ascribed above is valid, the difference should not be observed. The fact that the difference does appear suggests that other factors control the formation of the higher-valency oxides as well.

The following factors may influence the formation of the higher-valency oxides: 1) The sintered body prepared in the air presumably contained many cation vacancies.[3] The existence of vacancies is favorable for the ion movement in the crystal. 2) The gain in crystal-field stabilization energy on the chemisorption of oxygen on nickel oxide is high for the (110) face rather than the (100) face of the crystal.[20] This suggests that the (110) face is more active than the (100) face in the anodic oxidation. In the case of the sintered-body electrode, various crystal faces came in contact with the electrolyte. 3) Grain boundaries are considered to be high in surface free energy.[21] It has been pointed out that the surface free energy of a solid influences the rate of the anodic film formation process[22] as well as crystal growth.[23,24] Further study is necessary to elucidate which factor is most effective for the anodic oxidation of the nickel oxide crystal.

18) D. A. Vermilyea, "Advance in Electrochemistry and Electrochemical Engineering," Vol. 3, ed. by P. Delahay and C. W. Tobias, Interscience, New York (1963), p. 248.
19) J. F. Dewald, *J. Electrochem. Soc.*, **102**, 1 (1955).
20) J. Harber and F. S. Stone, *Trans. Farady Soc.*, **59**, 192 (1963).
21) E. Fujita, *Ōyō Butsuri*, **36**, 129 (1967).
22) D. A. Vermilyea, "Advance in Electrochemistry and Electrochemical Engineering," Vol. 3, ed. by P. Delahay and C.W. Tobias, Interscience, New York (1963), p. 223.
23) M. Fleishmann and H. R. Thirk, *Electrochim. Acta*, **2**, 22 (1960).
24) D. A. Vermilyea, *J. Chem. Phys.*, **25**, 1254 (1956).